WRINKLING OF STIFF FILMS ON STRETCHED COMPLIANT FILMS:

EXPERIMENTAL AND THEORETICAL STUDIES

A Thesis

by

YI YANG

Submitted to the Office of Graduate and Professional Studies of
Texas A&M University
in partial fulfillment of the requirements for the degree of

MASTER OF SCIENCE

Chair of Committee,	Ramesh Talreja
Committee Members,	Thomas W. Strganac
	Anastasia H. Muliana
Head of Department,	Rodney Bowersox

December 2013

Major Subject: Aerospace Engineering

ABSTRACT

Wrinkling of stiff film on semi-infinite compliant substrates has attracted attentions recently due to its important applications in stretchable electronics and micro-pattern metrology. However, wrinkling of a stiff film on a compliant thin film substrate has not been well understood. The composite bilayer comprised with a stiff film and a stretched film has a critical application in developing advanced thin film solar cells for long duration stratosphere balloons.

The presented thesis focuses on wrinkling of stiff films with finite widths on stretched compliant thin sheet via experimental and theoretical approach. Polyester films and low density polyethylene films have been utilized as the surface films and substrate films, respectively. Flexible polyvinyl chloride films has also been employed to serve as the surface layer for better understanding the physics behind the phenomena. The experiments reveal wrinkling phenomena of the film on the stretched thin sheet are very similar to that of a stiff film on a semi-infinite elastic foundation. A theoretical model considering finite width effect is formulated based on the concept of effective elastic foundation observed from the experiments via variational approach and principle of minimum potential energy. The results predicted by the theoretical model is validated via experiments and the finite width effect is also investigated and discussed.

In summary, the presented study shows the stretched film plays the role as a virtual semi-infinite elastic foundation for the surface film. The experimental observations and theoretical prediction of the phenomena has been achieved. It may provide a physics-based foundation for technology adventures in thin-film solar cell powered scientific balloon.

DEDICATION

Dedicated to my mother, wife, and daughter

ACKNOWLEDGEMENTS

NOMENCLATURE

LDPE   Low density polyethylene

PVC   Polyvinyl chloride

A wrinkling or buckling amplitude

B_c Bending rigidity of composite bilayer beam

D_f Flexural rigidity of plate/film

E_i Elastic modulus or Young's modulus, where $i = f,\ s,\ c$

   denoting film, substrate, and composite bilayer, respectively

$\bar{E}_i$ plane-strain elastic modulus

h_i film thickness, where $i = f,\ s$, denoting film, substrate, respectively

K_e effective stiffness of the virtual elastic foundation

L_1 Width of the substrate film and length of the surface film

L_2 Length of the substrate film

N_{ij} Axial force $(i = j)$ in i-direction or shear force $(i \neq j)$

T_3 Normal traction at the interface of the two layers

W Width of the surface film

ε_{ij} strain component follows N_{ij}

ε_{cr} critical buckling strain

κ Bending curvature

λ wrinkling or buckling wavelength

ν_i Poisson's ratio, where $i = f,\ s$, denoting film, substrate, respectively

ψ_b Bending energy density in film

ψ_m Membrane energy density in film if any

TABLE OF CONTENTS

LIST OF TABLES

1. INTRODUCTION

The first chapter of this thesis introduces background, motivation, and wrinkling phenomena for the current study. A large literature exists reporting short wavelength buckling/post-buckling wrinkles of compressed thin film attached to thick complaint substrate. However, very limited studies have been done on compressed film rested on thin soft substrate, especially compressed film bonded to stressed/stretched film. The goal of this thesis is to understand the mechanical behaviors of a stiffer elastic film bonded to a stretched soft elastic film with the potential to promote advances of new technology in developing sustainable energy system for long duration scientific balloons.

1.1   Background and Motivation

Membrane and film structures are widely used in deployable space structure applications such as stratospheric balloons, airships, solar sails and inflatable reflectors (Deng, 2012; Khoury, 2012; Zheng, 2009). Such type of structures can also be widely found in energy applications, especially in solar energy harvesting systems (Chopra et al., 2004; Lee et al., 2012), as well as in flexible and stretchable electronics (Khang et al., 2006; Kim et al., 2010), just to mention a few. Figure 1.1 shows several examples of the applications mentioned above.

Employing scientific balloon to Mars and Titan as a low cost approach to conduct cutting edge science has been studied for years (Hall et al., 2007; Hall, 2011). Another innovative idea of operating a network of high altitude balloons as effective as a network of satellites for certain communication objectives was proposed recently (Azevedo et al., 2011).   However, one big challenge for such tasks would be how to provide sustainable power supply to the devices carried by a balloon. Based on
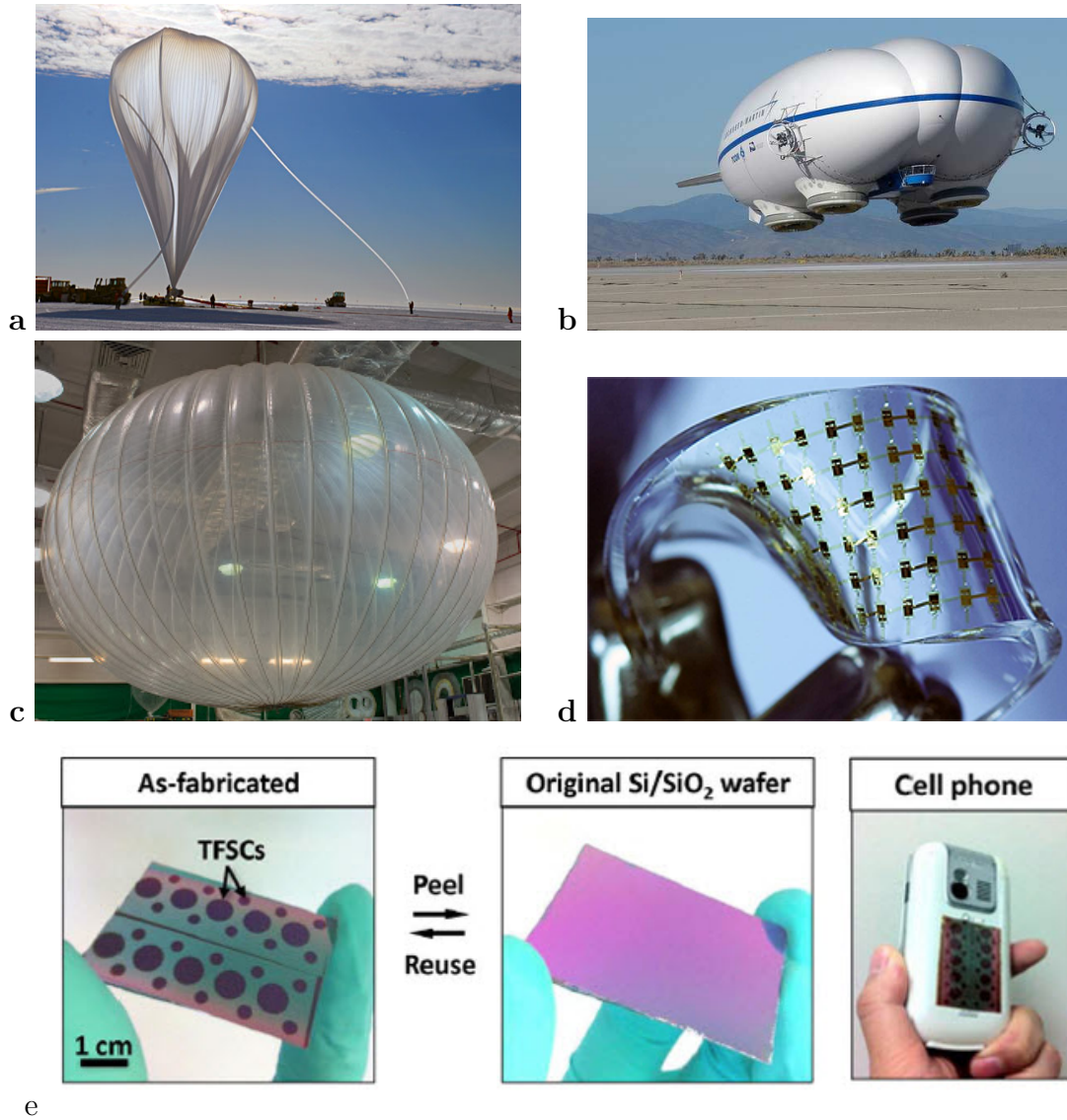
Figure 1.1: Application of membrane and film structures. (a) Zero pressure strato-spheric balloon (courtesy of NASA), (b) Lockheed Martin hybrid airship (courtesy of Lockheed Martin),(c) super pressure stratospheric balloon prototype (courtesy of NASA), (d) stretchable electronics (Kim et al., 2010), (e) thin film solar sticker (Lee et al., 2012).

the working environment of the balloon, the most convenient energy resource is solar energy which is clean and sustainable. To meet the light-weight requirement, and to collect enough power for balloon and device operation, there will be a minimum surface area required for the solar cell. Therefore, to balance these aspects mentioned, thin-film solar cell has attracted attentions. An effective approach proposed by the author is to stick thin strip of solar cell (Lee et al., 2012) onto the surface of balloon. The set of strip-like thin-film solar cells can be placed along either the longitude direction (referred to as machine direction) or the latitude direction (called transverse direction).

The solar film and balloon together comprise a composite bilayer system. Variation in thermal and mechanical loading condition (i.e. film temperature and pressure) will change the volume of the balloon and vary the strain in the bilayer. A distinct buckling phenomenon may occur when the shape of balloon changes due to applied loads. Sufficiently large compressive strain induced by the balloon membrane would generate surface wrinkling on the top layer due to the difference in the stiffness of the two layers. As a result, buckling of the thin-film solar cell may decrease the performance or even damage the solar cell. Understanding the formation of wrinkles and their incremental deformation with the increase of compressive strain on the film attached on stretched film is highly desirable to evaluate the proposed bilayer system.

1.2   Critical Review of Wrinkling Phenomena

Wrinkling is a phenomenon commonly observed in nature and industrial applications. Understanding this phenomenon from the point of view on instability dates back to several decades. In the middle of the last century, wrinkling analysis was applied to laminates in the form of sandwich panels comprised of two stiffer thin

sheets bonded to a thick soft core (Allen, 1969). In fact, the exploration of wrinkles in nature and in the art is an old subject, but the scientific study of wrinkles is a more recent developing area as it involves instabilities and large deformations in multiple-length-scales, as shown in Figure 1.2.

Wrinkling phenomena have been recently studied extensively both experimentally and theoretically (Brau et al., 2011, 2013; Cao and Hutchinson, 2012; Huang, 2005; Huang et al., 2005; Jiang et al., 2007, 2008; Pocivavsek et al., 2008; Sun et al., 2012). Among all classes of wrinkling phenomena, wrinkling of stretched/sheared sheet (Cerda and Mahadevan, 2003; Davidovitch et al., 2011; Puntel et al., 2011; Wong and Pellegrino, 2006a,b) and wrinkling of stiff film on complaint substrate (Cao and Hutchinson, 2012; Chen and Hutchinson, 2004; Groenewold, 2001; Huang et al., 2005; Huang, 2005; Shield et al., 1994; Song et al., 2008; Zang et al., 2012) are two representative categories.

1.2.1 Wrinkling of Stretched Sheet

Thin films are among the ubiquitous examples of flexible structures widely applied in aerospace, biomedical, and civil engineering. Tensional/stretching wrinkling in thin sheet, as shown in Figure 1.2(a), is intensively investigated and experimentally, analytically, and numerically (Cerda et al., 2002; Cerda and Mahadevan, 2003; Davidovitch et al., 2011; Puntel et al., 2011; Nayyar et al., 2011). In addition, pure shearing induced wrinkling also attracts attentions and has been studied recently (Massabò and Gambarotta, 2007; Wong and Pellegrino, 2006a,b). Pure shearing of an infinitesimal body can be considered as stretching in its two principal directions. Hence, shearing induced wrinkles have a similar mechanism as stretching induced wrinkles.

To understand wrinkling, two approaches, tension field theory (Coman, 2007;
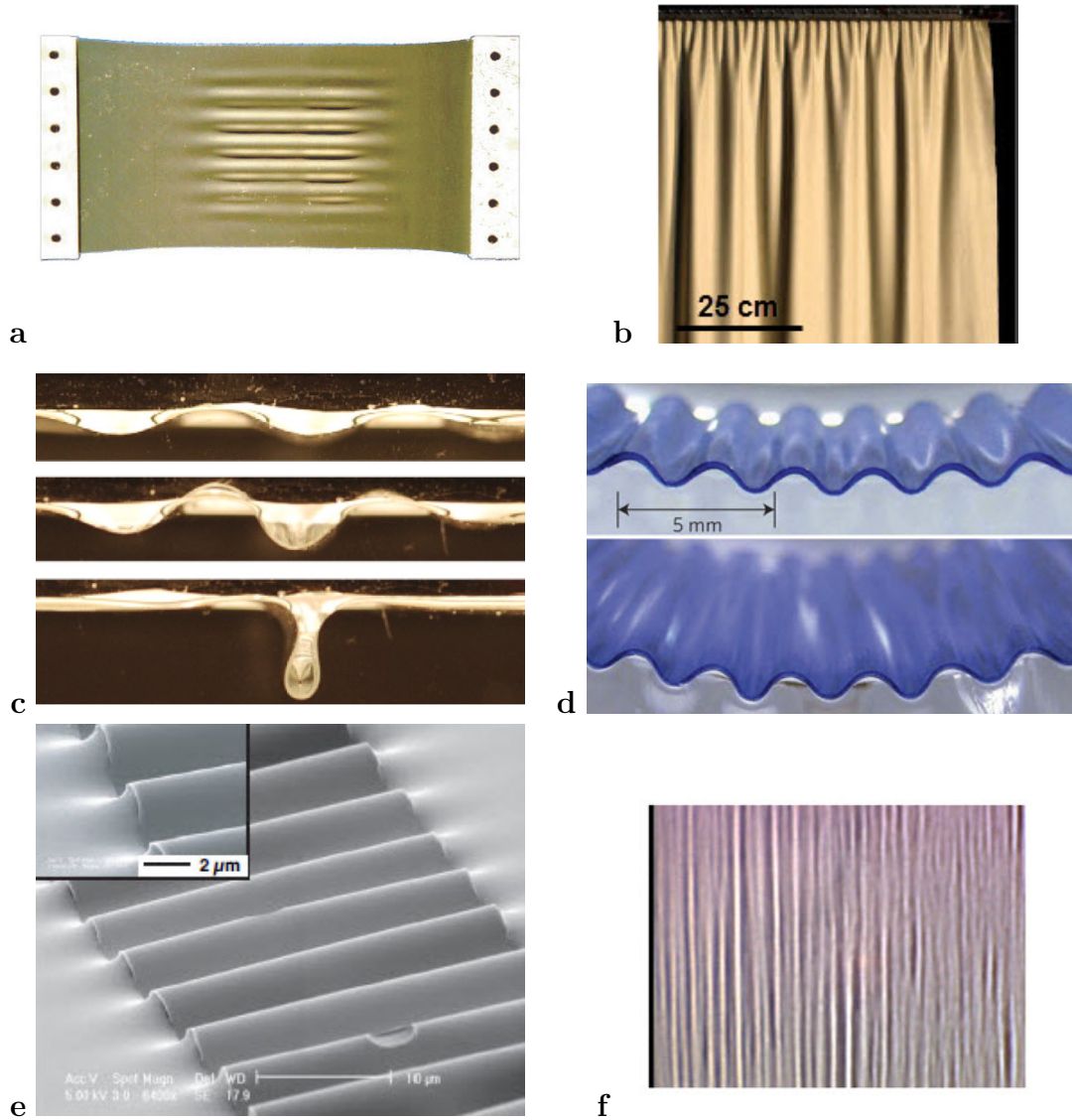
Figure 1.2: Multiple-length-scales in wrinkling phenomena. (a) Wrinkles in a polyethylene sheet (Cerda et al., 2002). (b) Pattern of folds obtained for a rubber curtain (Vandeparre et al., 2011). (c) Polyester film on water with wave length of 1.6 cm (Pocivavsek et al., 2008). (d) A thin coloured stiff PDMS film rested on a thick soft PDMS substrate (Brau et al., 2011). (e) Wrinkles in single-crystal Si ribbons attached to a PDMS substrate (Jiang et al., 2007). (f) Trilayer of colloidal gold nanoparticles on water with wavelength of 10μ m (Pocivavsek et al., 2008).

Steigmann, 1990) and bifurcation analysis (Nayyar et al., 2011; Zheng, 2009), have been commonly employed to analyze wrinkling of elastic membranes. Typically, tension field theory method can provide the prediction of the stress distribution and wrinkling regions. However, it may not provide wrinkle wavelength and amplitude. The bifurcation analysis are typically performed via nonlinear finite element method using thin shell theory. By employing this approach, critical condition for buckling and post-buckling may be obtained. For some simple cases, analytical solution can be obtained (Puntel et al., 2011; Wong and Pellegrino, 2006b).

Additionally, Cerda and Mahadevan (2003) provided the simple scaling analysis for uniaxial stretched polyethylene film and extended it for a wide range of wrinkling phenomena. Their approach has a distinguishing feature that the potential energy is minimized under a geometric constraint to solve the boundary value problem for the stretched sheet. The wrinkle wavelength λ and amplitude A were found to be

$$\lambda = 2\sqrt{\pi} \left(\frac{B}{T}\right)^{1/4} L^{1/2} \sim \left(\frac{B}{T}\right)^{1/4}, \tag{1.1}$$

and

$$A = \lambda \frac{\sqrt{2}}{\pi} \left(\frac{\Delta}{W}\right)^{1/2} \sim \lambda \left(\frac{\Delta}{W}\right)^{1/2}. \tag{1.2}$$

where B is the bending stiffness, T is the applied tensile load, L and W are the length and width of the film, respectively, Δ is the imposed compressive transverse displacement. Eq.(1.1) shows that wavelength of wrinkles decreases with the increase of applied strain. It is in good agreement with later numerical studies (Zheng, 2009; Nayyar et al., 2011). However, these later studies showed that the amplitude of wrinkles exhibits a non-monotonic dependence on the applied longitudinal strain.

Comparing the above equations with the corresponding solutions of beam buck-

ling on elastic foundation (Kármán and Biot, 1940), it is indicated that tensile force T plays a role as the "effective" elastic foundation for the stretched sheet. With the increase of T, the "effective" stiffness of the elastic foundation increases monotonically. Cerda and Mahadevan (2003) also suggested that the effective stiffness of this "virtual" foundation can be scaled as $K \sim T/L^2$. Details on the effective stiffness will be discussed in Chapter 3.

1.2.2 Wrinkling of Stiff film on Compliant Substrate

Stiff thin film rested on complaint substrate may suffer from wrinkling induced by the in-plane compression. It is similar to a classical problem in soil-structure interaction, buckling of beam/plate on elastic foundation. It has been pointed out that wrinkling may cause interfacial delamination (Mei et al., 2011; Shield et al., 1994; Vella et al., 2009). Most of the studies on this type of wrinkling assumes that the bonding between surface layer and substrate is sufficiently strong, such that buckling induced delamination is avoided. In the conventional analysis on wrinkling of stiff film bonded to compliant substrate, surface effects are neglected. However, it should be noted that surface properties will play an important role in nano-scale analysis (Huang et al., 2007).

Wrinkling of stiff film on soft substrate can be described using either an equilibrium approach (Huang, 2005; Huang and Suo, 2002; Im and Huang, 2005) or an energy method (Brau et al., 2011, 2013; Jiang et al., 2008; Pocivavsek et al., 2008; Song et al., 2008). It involves a balance of force/energy between film bending which suppresses short wavelengths, and substrate deformation which suppresses large wavelength. Most examples in the literature formulate the problem as a thin plate (Föppl von Kármán plate theory) or an Euler beam (considering large deflection) attached to a semi-infinite substrate (plain-strain condition), as illustrated in

Figure 1.3.

Figure 1.3: Schematic of an elastic film wrinkling on a compliant substrate (Huang et al., 2007)

The governing equation for the bending of a stiff film on a more complaint elastic substrate shown in Figure 1.3 is

$$\frac{\bar{E}_f h^3}{12}\frac{d^4 w}{dx^4} + N\frac{d^2 w}{dx^2} + K_w w = 0 \tag{1.3}$$

$\bar{E}_i = \frac{E_i}{(1-\nu_i^2)}$ is the plain-strain modulus, where the subscript i can be replaced by f or s, denoting the film and substrate, E is the Young's modulus; h is the thickness of the film, ν is the Poisson's ratio, K_w is the Winkler's modulus of an elastic semi-infinite foundation (Biot, 1937), $K_w = \bar{E}_s \pi/\lambda$, N is the applied compressive force, and λ is the wrinkle wavelength. The x-axis is defined to be parallel to the compression direction and the z-axis is perpendicular to the film surface. The solution of above equation has a sinusoidal form, thus, it is reasonable to assume that the deflection of the film can be described as:

$$w(x) = A cos\frac{2\pi x}{\lambda} \tag{1.4}$$

where A is the amplitude of wrinkle, $2\pi/\lambda$ is the so-called wave number. Substituting

8

Eq.(1.4) into Eq.(1.3) and solving for the applied force N yields

$$N = \frac{\bar{E}_f h^3}{3} \left(\frac{\pi}{\lambda}\right)^2 + \frac{\bar{E}_s \lambda}{4\pi} \tag{1.5}$$

From Eq.(1.5), it is clear that F is a function of λ. Setting $\partial F/\partial \lambda = 0$ gives the wavelength which minimizes the applied force N. The initial wrinkling (buckling) wavelength and its corresponding critical strain is the following.

$$\lambda_c = 2\pi h \left(\frac{\bar{E}_f}{3\bar{E}_s}\right)^{1/3} \tag{1.6}$$

and

$$\varepsilon_c = \frac{1}{4} \left(\frac{3\bar{E}_s}{\bar{E}_f}\right)^{2/3} \tag{1.7}$$

It is noted that the critical strain of wrinkling (ε_c) only depends on the modulus ratio of the substrate to film. When the applied strain exceeds the critical strain of initial wrinkling, post-buckling behavior will involve in the wrinkling process. For post-buckling, further strain is accommodated by increasing wrinkle amplitude, while wavelength remains constant. Although it has been shown that wavelength will decrease with increase of applied strain (Jiang et al., 2007), above conclusion is still valid and has been widely applied for film with small deformation. As indicated in Eq.(1.5), λ is independent of ε. When this holds true, at the instability threshold, the release of strain in the bilayer is represented by $\varepsilon - \varepsilon_c$, and a kinetic relation over one period of the wavelength can be expressed as

$$\varepsilon - \varepsilon_c = \frac{1}{\lambda} \int_0^\lambda \sqrt{1 + \left(\frac{dw}{dx}\right)^2} \, dx - 1. \tag{1.8}$$

Here, dw/dx is small. Expanding the above equation and only keeping the

quadratic term, and inserting in Eq.(1.4), gives

$$\varepsilon - \varepsilon_c = \frac{1}{\lambda} \int_0^\lambda \left(1 + \frac{1}{2}\left(\frac{dw}{dx}\right)^2 + ...\right) dx - 1 = \frac{\pi^2 A^2}{\lambda^2}. \tag{1.9}$$

Then, the expression connecting wrinkle amplitude and applied strain is obtained by combining Eq.(1.6), Eq.(1.7), and equation above, as

$$A(\varepsilon) = h\sqrt{\frac{\varepsilon}{\varepsilon_c} - 1}. \tag{1.10}$$

The critical strain at which wrinkling occurs, wrinkle amplitude and wavelength as a function of applied strain characterize the physics of the surface wrinkling phenomena. The above derivation and solutions for critical wavelength and strain are referred to as the conventional analysis for buckling of stiff film on complaint substrate without pre-stretching (Chung et al., 2011).

In the conventional analysis, the nonlinearity and incremental stiffness of the substrate is accounted by taking E_s as a function of λ. However, the nonlinearity due to pre-stretch has not been described. With pre-stretched substrate, the incremental modulus has a significant effect on the nonlinearity relevant to wrinkling (Hutchinson, 2013; Sun et al., 2012). Hutchinson (2013) investigated the role of nonlinear substrate elasticity in the wrinkling of thin films. The incremental modulus is precisely described. It identifies two dimensionless parameters that control the stability and mode shape of evolution of the bilayer. One parameter specifies arbitrary uniform substrate pre-stretch. Another is a stretch-modified modulus ratio. The effect of pre-stretch on bilayer of neo-Hookean material has been discussed by Cao and Hutchinson (2012). Song et al. (2008) studied wrinkling of elastic film on pre-stretched neo-Hookean substrate under large deformation. The nonlinearity of

10

the substrate can also be introduced by taking viscous layer (Huang and Suo, 2002) or viscoelastic layer (Huang, 2005; Im and Huang, 2005) as the substrate.

In addition to the initial wrinkling (buckling) described above, post-buckling behavior such as creasing, folding, and periodic doubling may occur (Brau et al., 2011, 2013; Sun et al., 2012). Brau et al (2013) also investigated the influence of the substrate nonlinearity on wrinkle to fold transition.

A complete review of the different types of wrinkling phenomena is out the scope of the thesis. Only the relevant of the background for the presented thesis is described here. Some detailed review on previous studies are discussed in each chapter.

1.3 Goal and Outline of the Thesis

The goal of the thesis is to investigate the wrinkling of compressed thin film bonded to a stretched film and to develop an approximate theoretical model to predict the phenomena. The compressive strain in the bilayer film is generated by Poisson contraction effect.

The thesis is organized as follows. Chapter 2 elaborates *in situ* experimental investigations of the wrinkling phenomenon in several bilayer systems using different polymeric materials. The physics-based theoretical model is developed via variational method and principle of minimum potential energy in Chapter 3. In Chapter 4, comparisons between prediction of wavelength from the theoretical model and experimental measurement are performed. Finally, conclusions are drawn from the findings, with recommendations for the future directions given in Chapter 5.

2. EXPERIMENTAL OBSERVATIONS

Buckling and post-buckling wrinkle patterns are generated experimentally in a group of polyester films as well as a group of flexible polyvinyl chloride (PVC) film attached to a stretched low density polyethylene (LDPE) thin film. The lateral compressive strain induced by Poisson effect is provided by stretching the substrate film. Wrinkle patterns are observed with significant differences compared with wrinkling of the stretched sheet, and exhibit a similar behavior as wrinkling of stiff film on compliant substrate. It is also found that the width of the surface layer significantly affects the formation of wrinkle patterns.

2.1 Experimental Description

The aim of the presented experiments is to observe the wrinkling phenomena when a stiff elastic film is attached to a stretched soft elastic film. The experimental observations may provide a foundation for physics-based modeling or simulation.

Two groups of surface film are tested. One is flexible polyvinyl chloride (PVC) film purchased from 3M® and another is polyester film. The substrate layer is low density polyethylene (LDPE) film. Both polyester and LDPE film are purchased from McMaster-Carr®. Materials are selected based on the differences in elastic modulus that $E_{flexiblePVC} < E_{LDPE} < E_{polyester}$. Table 2.2 and Table 2.1 summarize the material properties and geometries of the films used in the experiments.

It is known that wrinkles can be introduced by stretching a thin sheet, which is undesired in the current experiments. It is favorable that wrinkles appearing on the surface layer are generated by buckling of surface layer rather than induced by the buckling of the substrate layer. A recent study (Nayyar et al., 2011) indicated that wrinkling of stretched rectangular sheet can be suppressed by controling the thickness

12

Table 2.1: Geometries of utilized thin films

Material	Length (mm)	Width (mm)	Thickness (mm)
LDPE	145	40	0.1
Polyester	40	2.5, 10, 20, 40	0.05
Flexible PVC	40	2.5, 10	0.15

Table 2.2: Material properties of the employed films

Materials	Young's Modulus (GPa)	Poisson's Ratio
LDPE	0.3	0.44
Polyester	$4.9 \sim 5.1$ (select 5.0)	0.38
Flexible PVC	$\ll 0.3$	N/A

and the aspect ratio (ratio of length over width). Their results suggested that wrinkle amplitudes will be much smaller than the thickness of the film if width/thickness$\simeq$ 1000 and the aspect ratio $\simeq$ 3.2. Thus, sizes of the substrate film shown in Table 2.1 were carefully selected based on the conclusions drawn from Nayyar et al. (2011), such that wrinkles are aimed to be suppressed.

Figure 2.1 shows simple wrinkling tests on two stretched LDPE films. Both films have the same material properties and geometry except thickness. Along the transverse direction, black lines are marked using marker pen for clear observation. It is observed that upon the stretch ratio reach 1.2 (current length/original length), no wrinkles can be observed in the sheet with 0.1 mm thickness and an aspect ratio of 3.6. However, wrinkles are clearly observed in the one with 0.05mm thickness. Therefore, the substrate film is selected as listed in Table 2.1.

A built-in-house uniaxial stretching apparatus was employed to perform the test, as shown in Figure 2.2. Film was clamped at its ends. It was found in previous works that stress field and deformation in clamped film under uniaxial stretching
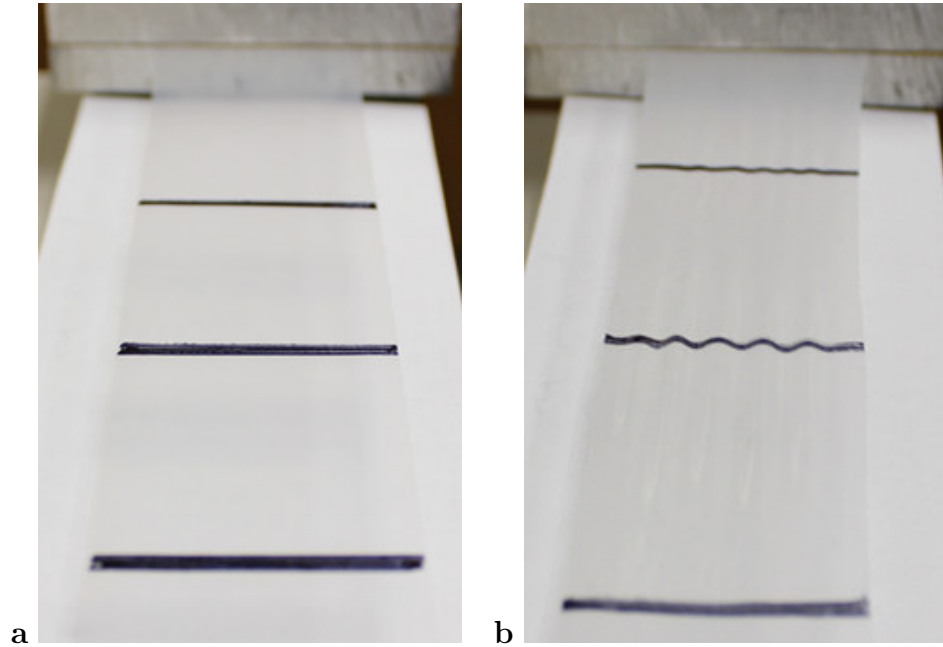
Figure 2.1: Wrinkling suppression of stretched rectangular LDPE film. (a) LDPE film with 145 mm long, 40 mm wide and 0.1 mm thick. (b) LDPE film with 145 mm long, 40 mm width and 0.05 mm thick.

is inhomogeneous (Cerda et al., 2002; Nayyar et al., 2011). Therefore, the lateral contraction due to Poisson effect is also inhomogeneous. The mid-section of the substrate along the longitude direction has the largest lateral contraction. Thus, the surface film will be attached on the mid-section of the substrate as shown in Figure 2.2. In the experiments, displacement was applied by manually controlling the sliding block via the screw.

The substrate film was cut into pieces and gently cleaned and flattened. Then, surface film was mounted on the mid-section of the substrate. After that, bilayer was clamped at the two ends on the test apparatus. There was no pre-stretch induced during the process. Then, the film/substrate composite was subjected to incremental compression by increasing the longitude displacement. During the tests, measurements on displacement, wavelength and lateral contraction were carried out by a
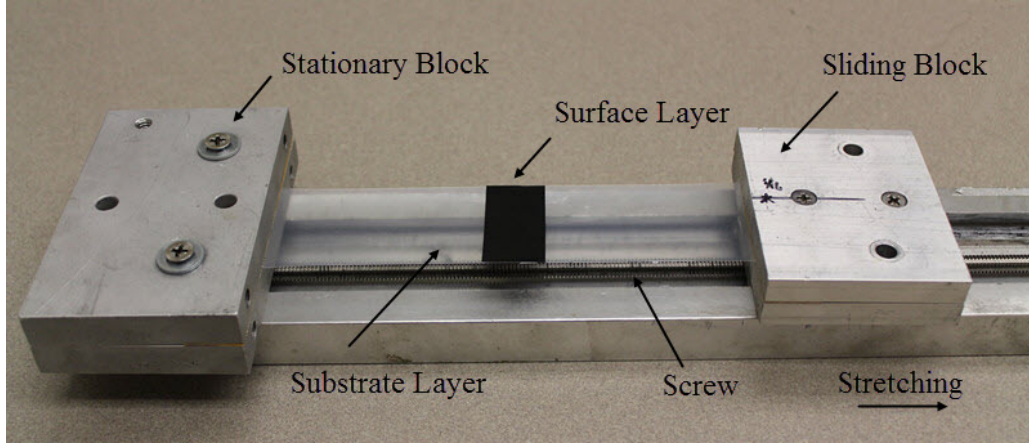
Figure 2.2: Experimental setup

precision vernier caliper with the accuracy of 0.25 mm.

Tensile or compressive strain mentioned in the thesis are defined as nominal strain or overall strain, $\varepsilon_{22} = \frac{L_2 - L_{02}}{L_{02}}$ and $\varepsilon_{11} = \frac{L_1 - L_{01}}{L_{01}}$, where L_2 and L_1 are the current length and width, respectively, and L_{02} and L_{01} are the original length and width, respectively. After wrinkles formed, the evolution of wrinkle wavelength with increasing compressive strain was recorded via a digital SLR camera. The influence of width effect on wrinkle patterns was also investigated.

2.2 Formation and Evolution of Wrinkles

Formation of wrinkles, called initial wrinkling here, is considered as buckling phenomena, while evolution of wrinkles is considered as a post-buckling behavior. In the experiments, it was found that the employed polyethylene film remains elastic until the tensile nominal strain reaches approximately 20%. Observations from the experiments are displaced in Figure 2.3 and Figure 2.4.

Figure 2.3 shows wrinkle formation and evolution on the flexible PVC/LDPE composite bilayer. The wavelength decreases with increases in compressive strain, while the wrinkle amplitude increases with the growth of compressive strain. These
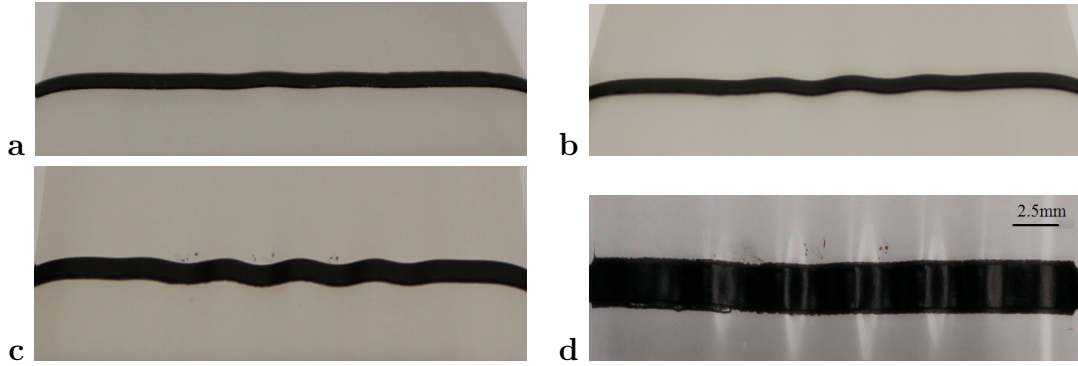
Figure 2.3: Wrinkling of 2.5 mm wide flexible PVC film. (a) initial wrinkles at $\varepsilon_{11} = 7.1\%$, (b) wrinkles at $\varepsilon_{11} = 8.8\%$, (c) wrinkles at $\varepsilon_{11} = 10.7\%$, (d) wrinkles at $\varepsilon_{11} = 12.4\%$ (top view).

Figure 2.4: Wrinkling of 2.5 mm wide polyester film. (a) initial wrinkles at $\varepsilon_{11} = 0.31\%$, (b) wrinkles at $\varepsilon_{11} = 1.6\%$, (c) wrinkles at $\varepsilon_{11} = 2.1\%$, (d) wrinkles at $\varepsilon_{11} = 6.1\%$ (top view).

observations agree well qualiyatively with the finite deformation analysis of buckled film on complaint substrate by Jiang et al. (2007). In Figure 2.3 (d), deformation has exceeded the elastic range, and slight interfacial debonding can be observed. Due to experimental limitations, it was not possible to perform amplitude measurements in addition to wavelength measurement.

The polyester films purchased here are transparent. Hence, they are colored manually by blue marker pen along their length for clear observations. Similar to the previous case, the wavelength decreases with increases in compressive strain, while the wrinkle amplitude increases with the growth of compressive strain. Comparing Figure 2.4 with Figure 2.3, it is found that the critical strain at which wrinkle forms for polyester/LDPE bilayer is much smaller than that of flexible-PVC/LDPE bilayer. This is due to the different elastic modulus of two materials. It can be concluded that film with a lower elastic modulus will have a higher critical buckling strain. This conclusion again agrees with the conventional analysis indicated in Eq.(1.7). Another interesting phenomenon one may observe is that the wrinkle in the center has a larger amplitude than its neighbours'. Evolution of wrinkles starts from the center of the surface layer, then propagates along the length. This phenomenon can also be observed in wider films discussed later.

2.3   Finite Width Effect

In the previous chapter, it was mentioned that the conventional analysis involved a critical assumption that the surface film width is much larger than the wavelength such that the deformation was under plain strain condition. However, this may not hold for a stripe-like film. Recent works (Jiang et al., 2008; Tarasovs and Andersons, 2008) pointed out that the wrinkle wavelength and amplitude also depends on the film width when the film is moderately narrow. In this section, the width effects are

Figure 2.5: Wrinkling of 10 mm wide polyvinyl film. (a) initial wrinkles at $\varepsilon_{11} = 4.8\%$, (b) wrinkles at $\varepsilon_{11} = 6\%$ (top view), (c) wrinkles at $\varepsilon_{11} = 8.9\%$, (d) wrinkles at $\varepsilon_{11} = 10.7\%$.

experimentally investigated for the two composite bilayers. Two cases (one for each) are photographed as typical cases for illustration.

Evolution of wavelength and amplitude follows the same trend as found in the narrower film observed in previous section. Comparing Figure 2.5 with Figure 2.3, it can be observed that the narrower film has a higher critical strain, whereas, the wider film has a larger wrinkling wavelength. This also agrees with the experimental observations and theoretical analysis by Jiang et al. (2008) and Tarasovs and Andersons (2008) on semi-infinite substrate. The buckling occurs starting from the center of the film which is similar to what was observed in the narrower film. As shown in Figure 2.5 (b), wrinkle in the center has a larger amplitude than its neighbours. With the increase of compressive strain, the neighbour wrinkles grow at the expense of delaying the central wrinkle's growth. Finally, amplitude and wavelength of each wrinkle approach the same value through the length of the surface layer. Note that, slight delamination can be observed at the edge far from the view in Figure 2.5 (d). In addition, wrinkling of 10 mm wide polyester film behaves the same way as
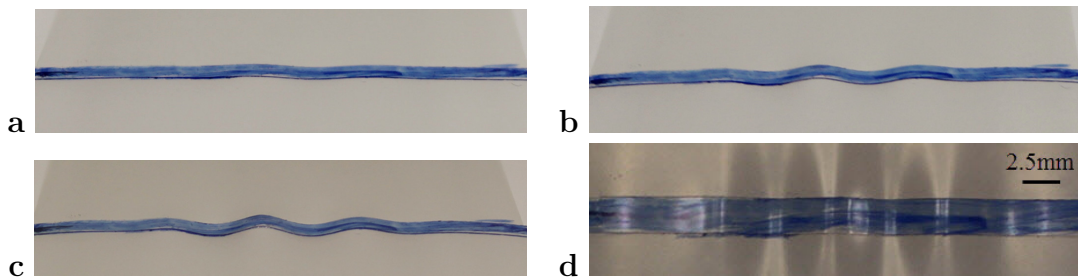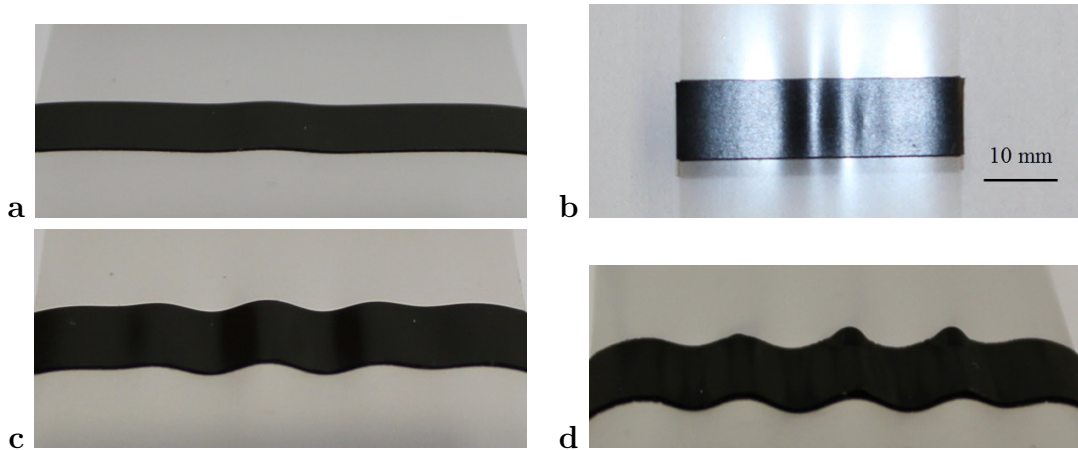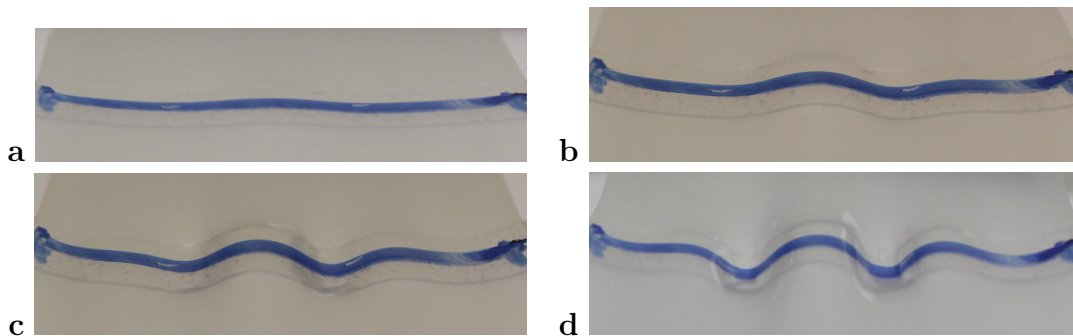
Figure 2.6: Wrinkling of 10 mm wide polyester film. (a) initial wrinkles at $\varepsilon_{11} = 0.4\%$, (b) wrinkles at $\varepsilon_{11} = 1.9\%$, (c) wrinkles at $\varepsilon_{11} = 4.1\%$, (d) wrinkles at $\varepsilon_{11} = 6.7\%$.

wrinkling of 10 mm wide flexible PVC shown in Figure 2.6.

2.4 Summary of Observations

In the beginning of this chapter, it was motioned that $E_{flexiblePVC} < E_{LDPE} < E_{polyester}$. Thus, two bilayer systems were: a compliant film on a stiff substrate and another a stiff film on a complaint substrate. Wrinkle wavelength as a function of compressive strain for each surface layer with varying width is plotted in Figure 2.7

From Figure (2.7), observations can be summarized as the following. Wavelength decreases with increase of compressive strain monotonically in each case studied. For the same width, a film with smaller elastic modulus has a smaller wrinkle wavelength and larger critical buckling strain. For the same material, a wider film has a larger wavelength at the same strain. These conclusions agree well with the conventional analysis on wrinkling of stiff film bonded to compliant substrate by many previous works as mentioned in Chapter 1.

Results from the experiments show that wrinkling mechanism of thin-film on stretched thin-film is very similar to wrinkling of thin-film attached on semi-infinite elastic substrate. And these observations may suggest that the stretched film or the tensile strain in the substrate may play a role as an equivalent elastic foundation.

The analogy on the effective elastic foundation for a stretched sheet suggested by Cerda and Mahadevan (2003) is experimentally shown in this chapter.
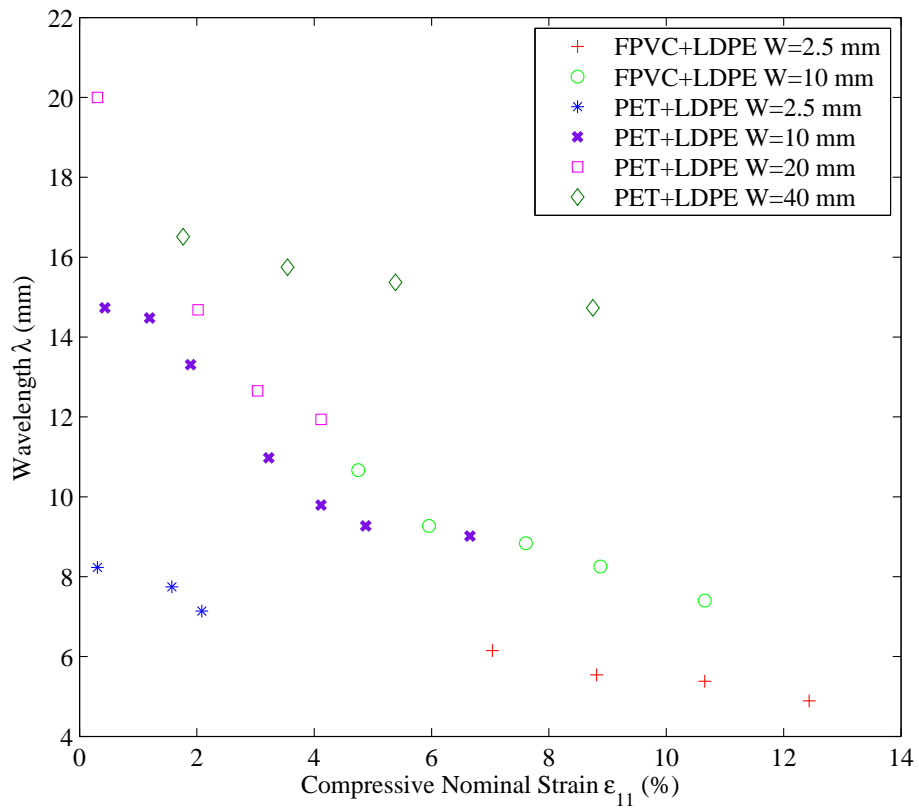
Figure 2.7: Wrinkle wavelength as a function of applied compressive strain for specimens with varying width (FPVC represents flexible PVC, and PET represents polyester).

3. MODEL FORMULATION

A theoretical model is formulated in this chapter. Lagrangian description is utilized to describe the deformation of the material points of the film. The surface layer is modeled as a nonlinear von Kármán plate with small strain but large deflection. The substrate is modeled as a thin elastic sheet under uniaxial tension. Here, the tension is considered quasi-statically applied. The governing equation of the wrinkle formation is then obtained by variational approach. Corresponding solutions for critical conditions are achieved by minimization of potential energy.

3.1 Kinematics

The problem is formulated in the continuum scale. It is assumed that the composite bilayer film can be viewed as having a continuous distribution of matter in space and time. The bilayer is imagined as being composition of a continuous set of material points. The deformation of the bilayer film is illustrated in Figure 3.1.

$\mathbf{x}(x_1, x_2, x_3)$ is the position vector, and $\mathbf{u}(\mathbf{x})$ is the displacement field (u_1, u_2, u_3) or
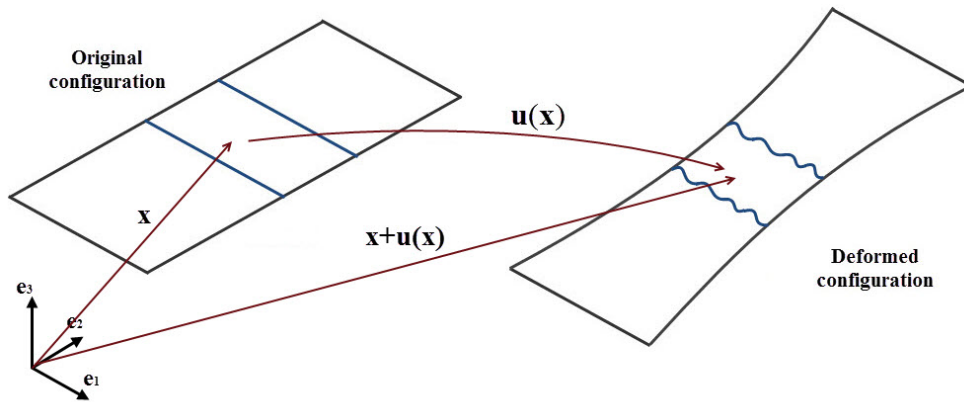
Figure 3.1: Deformation of the composite bilayer by continuum mechanics

(u, v, w). The corresponding displacement gradient $(grad\ u)$ and deformation gradient (F_{ij}) are formulated by classical continuum theory (Bower, 2010)

$$grad\ u = \frac{\partial u_i}{\partial x_k}, \ \ F_{ik} = \delta_{ik} + \frac{\partial u_i}{\partial x_k} \tag{3.1}$$

where, δ_{ik} is the Kronecker delta and subscripts i, j, k take values 1, 2, and 3. In the presented problem, Lagrange strain tensor is utilized.

$$E_{ij} = \frac{1}{2}(F_{ki}F_{kj} - \delta_{ij}) = \frac{1}{2}\left(\frac{\partial u_i}{\partial x_j} + \frac{\partial u_j}{\partial x_i} + \frac{\partial u_k}{\partial x_j}\frac{\partial u_k}{\partial x_i}\right) \tag{3.2}$$

Consider the substrate is a rectangular sheet with width of L_1, length of L_2, and thickness of h_s. And the surface film is also a rectangular sheet with width of W, length of L_1, and thickness of h_f. Choose a reference coordinate such that

$$x_1 \in [-\frac{L_1}{2}, \frac{L_1}{2}], \ \ x_2 \in [-\frac{L_2}{2}, \frac{L_2}{2}], \ \ x_3 \in [-h_s, h_f] \tag{3.3}$$

Figure 3.2 shows the mid cross-section, in (x_1, x_3) plane, of the bilayer in the deformed configuration. Assume that the buckled film is inextensible and the deflection is $w(x_1)$, where x_1 denotes the coordinate in the reference configuration. Let ϕ denotes the angle between horizontal (dash line) and tangent $(\mathbf{t})$ at a point of the deformed surface film. Lagrangian description is adapted here, such that x_1 labels each material point in the deformed configuration. Because the problem is symmetric zbout the axis of symmetry, only half of the wrinkled bilayer is illustrated in Figure 3.2. Let $sin\phi = \partial w/\partial x_1 \doteq w_{,1}$, then, $cos\phi(\partial\phi/\partial x_1) = w_{,11}$, the following kinematic relations will hold.

$$\kappa = \frac{\partial\phi}{\partial x_1} = \frac{w_{,11}}{\sqrt{1 - w_{,1}^2}} \tag{3.4}$$
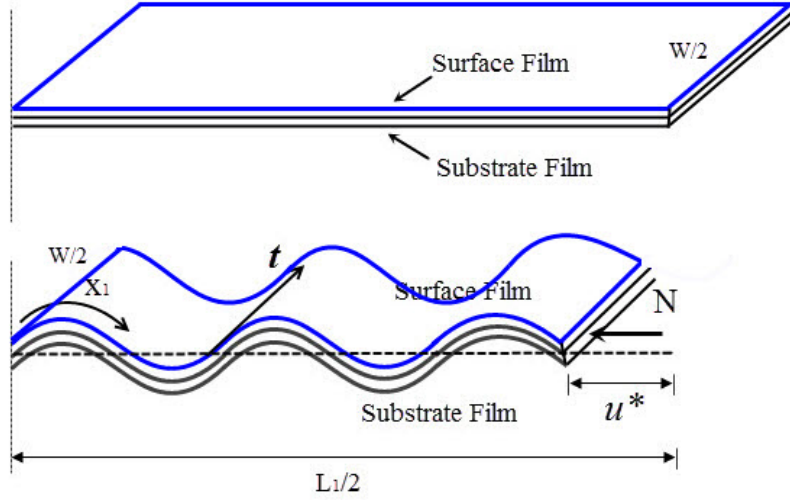
Figure 3.2: Schematic illustration of wrinkled bilayer. a pre-buckling state at top and a wrinkling state at the bottom

$$u^* = \frac{L_1}{2} - \int_0^{\frac{L_1}{2}} \sqrt{1 - w_{,1}^2}\,dx = \int_0^{\frac{L_1}{2}} (1 - \sqrt{1 - w_{,1}^2})\,dx \qquad (3.5)$$

Here, κ denotes the curvature. u^*, shown in Figure 3.2 is the compressed displacement along horizontal direction. Eq.(3.5) imposes the condition of extensibility to the composite system. This constraint for the system plays an important role in potential energy minimization.

3.2   Deformation of the Surface Film

The nonlinear von Kármán plate theory (Timoshenko and Woinowsky-Krieger, 1987; Landau and Lifshitz, 1959) for large deflection of thin elastic plate under in-plane and out-of-plane loads is employed for modeling of the surface layer. The two layers are considered to be bonded perfectly, such that delamination will be avoided. Then, the surface film is subject to the normal traction T_3, as well as, the shear traction T_1 and T_2. The displacement components are adapted as (u, v, w) as described in previous section. The in-plane strain is connected to the displacement

via Lagrange strain tensor, Eq.(3.2).

Since the material is assumed to be linear elastic material, the in-plane force and strain can be connected via linear elastic constitutive relations.

$$N_{\alpha\beta} = E_f h_f \left(\frac{\varepsilon_{\alpha\beta}}{1+\nu_f} + \frac{\nu_f}{1-\nu_f^2} \varepsilon_{\gamma\gamma} \delta_{\alpha\beta} \right) \tag{3.6}$$

where subscript f denotes film, subscripts α, β, γ take values 1 and 2. E_f is elastic (Young's) modulus, ν_f is Poisson's ratio, h_f is the thickness. The normal traction T_3 and shear traction $T_{\alpha\beta}$ at the interface of two layers can be obtained from the force equilibrium.

$$T_3 = D_f \frac{\partial^4 w}{\partial x_\alpha \partial x_\alpha \partial x_\beta \partial x_\beta} - N_{\alpha\beta} \frac{\partial^2 w}{\partial x_\alpha \partial x_\beta} - T_\alpha \frac{\partial w}{\partial x_\alpha} \tag{3.7}$$

$$T_\alpha = \frac{\partial N_{\alpha\beta}}{\partial x_\beta} \tag{3.8}$$

where $D_f = E_f h_f^3/12(1-\nu_f^2)$ is the flexural rigidity or bending stiffness of the surface film. The elastic energy in the deformed film includes two parts, membrane energy from in-plane deformation and energy generated by out-of-plane bending. The corresponding energy density equations are

$$\psi_m = \frac{1}{2} N_{\alpha\beta} \varepsilon_{\alpha\beta}, \tag{3.9}$$

and

$$\psi_b = \frac{D_f}{2} \left[\left(\frac{\partial^2 w}{\partial x_1^2} + \frac{\partial^2 w}{\partial x_2^2} \right)^2 - 2(1-\nu_f) \left(\frac{\partial^2 w}{\partial x_1^2} \frac{\partial^2 w}{\partial x_1^2} - \left(\frac{\partial^2 w}{\partial x_1 \partial x_2} \right) \right) \right]. \tag{3.10}$$

The total energy density is obtained by adding Eq.(3.9) and Eq.(3.10).

It is noted that if there is no variation in vertical displacement w along the width,

the partial differential equations became ordinary differential equations. Such that, the nonlinear plate theory reduces to the large deflection beam theory. Plane strain modulus is then replaced by Young's modulus. Then, the in-plane membrane force in the beam is

$$N_{11} = WE_f h_f \varepsilon_{11}, \tag{3.11}$$

with membrane strain

$$\varepsilon_{11} = \frac{du_1}{dx_1} + \frac{1}{2}\left(\frac{dw}{dx_1}\right)^2. \tag{3.12}$$

The normal traction and shear traction between the two layers are

$$T_3 = \frac{E_f W h^3}{12}\frac{d^4 w}{dx_1^4} - N_{11}\frac{d^2 w}{dx_1^2} - T_1\frac{dw}{dx_1}, \tag{3.13}$$

and

$$T_1 = \frac{dN_{11}}{dx_1}. \tag{3.14}$$

The energy density functions become

$$\psi_m = \frac{1}{2}N_{11}\varepsilon_{11}, \tag{3.15}$$

and

$$\psi_b = \frac{D_f}{2}\left(\frac{d^2 w}{dx_1^2}\right)^2. \tag{3.16}$$

If the film thickness is much smaller than any other characteristic lengths in the film, such as wrinkling wavelength, film width or length, then the film can be modeled using large deflection beam theory (Song et al., 2008; Zang et al., 2012). In the presented study, the thickness of both films are much smaller than other characteristic length, and there is no significant variation in the width direction of

the film, as been observed experimentally. Thus, the beam model can be adapted to adequately model the deformation of the surface film.

3.3 Stiffness of the Effective Elastic Foundation

As introduced in Chapter 1, Cerda and Mahadevan (2003) firstly developed a simple scaling law to describe the wrinkling phenomena of a stretched sheet. The sheet is shown in Figure 1.2 (a). Their analysis employed the principle of minimum potential energy. The bending energy due to deformation is predominant in the transverse direction along width. And the stretching energy due to applied tension is restored and released along the longitude direction. The selection of wrinkle wavelength is balanced between the bending energy and the stretching energy.

The stretching energy presented in their paper has the form of

$$U_s = \frac{1}{2} \int_A T(x)(\frac{\partial \zeta}{\partial x})^2 dA \tag{3.17}$$

where $\zeta(x, y)$ is the vertical deflection of the sheet, T is the tensile load, A denotes the sheet area. It is analogous to the form the energy in an elastic foundation supporting sheet (Landau and Lifshitz, 1986; Timoshenko and Woinowsky-Krieger, 1987),

$$U_F \sim \frac{1}{2} \int_A K\zeta^2 dA. \tag{3.18}$$

where K is the stiffness of the foundation. Therefore, one may consider the following scale relation may hold.

$$K_e \sim \frac{T}{L_2^2} \tag{3.19}$$

Here, K_e is designated as the stiffness of the "effective" elastic foundation. Then the stretched sheet can be imaged as a sheet rested on a virtual elastic foundation with

26

stiffness K_e. Here, the tensile load T (N_{22} in the presented work) can be scaled as $T \sim L_1 E_s h_s \varepsilon_{22}$. Therefore, the stiffness of the "effective" elastic foundation will be finally formed as

$$K_e = c_0 \frac{L_1 E_s h_s \varepsilon_{22}}{L_2^2} = c_0 \frac{L_1 E_s h_s \varepsilon_{11}}{\nu_s L_2^2} \tag{3.20}$$

where c_0 is the scale factor need to be determined, the minus sign "-" in conventional definition of Poisson's ratio is omitted. Inserting Eq.(3.11) into Eq.(3.20), the stiffness of effective elastic foundation can be obtained in terms of the lateral compressive force.

$$K_e = c_0 \frac{L_1 E_s h_s N_{11}}{L_2^2 E_c (h_s + h_f) W \nu_s} = c_0 \alpha N_{11} \tag{3.21}$$

where, $\alpha = \frac{L_1 E_s h_s}{L_2^2 E_c (h_s + h_f) W \nu_s}$.

It is noted that K_e is a linear function of the lateral compressive strain ε_{11} or force N_{11}. However, Eq.(3.12) indicates that K_e is a nonlinear function of the vertical deflection $w(x_1)$ or wavelength λ.

3.4   Formation of Wrinkles

With the preliminaries presented in the previous sections, the problem can be considered as a composite beam resting on a virtual elastic foundation. The equivalent bending modulus E_c and bending rigidity B_c of the composite beam are obtained as

$$E_c = \frac{1 + m^2 n^4 + 2mn(2n^2 + 3n + 2)}{(n + 1)^3 (1 + mn)} E_f \tag{3.22}$$

and

$$B_c = E_c \frac{W(h_s + h_f)^3}{12} = \frac{(E_f h_f^2 - E_s h_s^2)^2 + 4 E_f h_f E_s h_s (h_s + h_f)^2}{12(E_f h_f + E_s h_s)} W, \tag{3.23}$$

where, $m = E_s/E_f$, $n = h_s/h_f$. Following the approach of Koiter's instability analysis (van der Heijden, 2009), the potential energy per wavelength in the system shown in Figure 3.2 can be expressed as

$$\Pi = \frac{1}{\lambda} \int_0^\lambda \left(\frac{1}{2} B_c \frac{w''^2}{1 - w'^2} + \frac{1}{2} c_0 \alpha N_{11} w^2 \right) dx_1 \qquad (3.24)$$
$$- \frac{1}{\lambda} \int_0^\lambda N_{11}(1 - \sqrt{1 - w'^2}) dx_1$$

The first integral represents the energy from the system deformation, and the second integral represents the work done by the external load. It can also be considered as minimization of the deformation energy $\left(\frac{1}{2} B_c \frac{w''^2}{1-w'^2} + \frac{1}{2} c_0 \alpha N_{11} w^2 \right)$ subjected to the kinematic constraint $1 - \sqrt{1 - w'^2}$ with the Lagrange multiply N_{11}. Taylor's expansion gives

$$\frac{1}{1 - w'^2} = 1 + w'^2 + w'^4 + ... \qquad (3.25)$$

and

$$\sqrt{1 - w'^2} = 1 - \frac{1}{2} w'^2 - \frac{1}{8} w'^4 + ... \qquad (3.26)$$

Substitute the Taylor's expansion into Eq.(3.24), the potential energy functional then can be written as a summation of polynominal series with respect to w. It is sufficient to consider only the second order term in the polynominal, such that if the second order term Π_2 is positive-defined, the system will be stable. The limiting case that $\Pi_2(w) = 0$ for a nonzero displacement field is the critical case of neutral equilibrium. The second variation of the potential energy functional Π_2 are then given by

$$\Pi_2[w; N_{11}] = \frac{1}{\lambda} \int_0^\lambda \left(\frac{1}{2} B_c w''^2 + \frac{1}{2} c_0 \alpha N_{11} w^2 - \frac{1}{2} N_{11} w'^2 \right) dx_1 \qquad (3.27)$$

Consider a small variation ξ, and set the first variation of Π_2 to be zero, $\delta \Pi_2/\delta \xi =$

28

0, this gives the Euler-Lagrange Equation of the system as

$$B_c w'''' + N_{11} w'' + c_0 \alpha N_{11} w = 0, \tag{3.28}$$

which is the governing equation of the presented problem. Solution of the governing equation can be expressed by a Fourier sine/cosine series. From the experimental observations, it is reasonable to assume one solution of Eq.(3.28) has a simple form of

$$w(x_1) = A\cos\left(\frac{2\pi x_1}{\lambda}\right) = A\cos(kx_1), \tag{3.29}$$

where $k = 2\pi/\lambda$ is the wrinkling wave number. The above solution is also the assumed profile in many previous studies mentioned in Chapter 1. Substituting Eq.(3.29) into the governing equation gives

$$B_c k^4 - N_{11} k^2 + c_0 \alpha N_{11} = 0. \tag{3.30}$$

Solving above equation for the compressive force N_{11} yields,

$$N_{11} = \frac{B_c k^4}{k^2 - c_0 \alpha}. \tag{3.31}$$

By chain role,

$$\frac{dN_{11}}{d\lambda} = \frac{dN_{11}}{dk}\frac{dk}{d\lambda}, \tag{3.32}$$

therefore,

$$\frac{dN_{11}}{d\lambda} = 0 \implies \frac{dN_{11}}{dk} = 0. \tag{3.33}$$

This will lead to a wave number or wavelength that minimizes N_{11}. The admissible

critical wave number k_{cr} is then obtained as

$$k_{cr} = \sqrt{2c_0\alpha} \qquad (3.34)$$

And the corresponding wavelength of initial wrinkling is

$$\lambda_{cr} = \frac{2\pi}{k_{cr}} = \pi\sqrt{\frac{2}{c_0\alpha}}. \qquad (3.35)$$

Substituting Eq.(3.34) into Eq.(3.31) gives,

$$N_{cr} = 4B_c c_0 \alpha. \qquad (3.36)$$

And taking Eq.(3.11) into above equation, where E_f and h_f are replaced by E_c and $h_s + h_f$, respectively. Then, the critical compressive strain at which wrinkling occurs can be obtained as

$$\varepsilon_{cr} = \frac{4B_c c_0 \alpha}{W E_c(h_s + h_f)}, \qquad (3.37)$$

which can be expressed as

$$\varepsilon_{cr} = c_0 \frac{L_1 E_s h_s(h_f + h_s)}{3L_2^2 W E_c \nu_s}. \qquad (3.38)$$

4. MODEL VALIDATION

The developed theoretical model is validated here by physical experiments. A set of polyester films with different widths but with the same length and thickness are employed as the surface layer. LDPE film is still used as the substrate. Experimental setup and procedures are the same as in Chapter 2. Width effects on wrinkling profile are discussed. The prediction of the analytical model agrees with the experimental observations in scale without data fitting.

4.1   Experiment Measurements

Experiments were performed on polyester/LDPE bilayer. The substrate film has the exact dimensions as used in Chapter 2 (145 mm in length, 40 mm in width, and 0.1 mm in thickness). The surface layer, polyester film, was cut precisely with the exact geometry as Chapter 2 except variations in width. The widths of polyester film selected here are 2.5 mm, 5 mm, 7.5 mm, 10 mm, 12.5 mm, and 15 mm. Materials used in the experiments have the properties as listed in Table 2.2.

In the experiments, width is the only variable. Based on the width of each polyester film, tests were divided into six sets. To increase the sampling number, in each set of tests, initial wrinkling (buckling) wavelength and critical strain were measured for 5 to 7 times following the sequence, loading $\rightarrow$ measuring $\rightarrow$ unloading $\rightarrow$ relaxing $\rightarrow$ loading... The root mean square (RMS) value of each test set is considered as the representing value. Due to experiment limitations, only buckling wavelength can be measured accurately to some extent. Initial wrinkling wavelength was measured by measuring the peak-to-peak distance of the formed "valley or ridge". Such that, initial wrinkling wavelength can be obtained as a function of film width.

4.2 Validation

Recalling the expression derived for buckling (initial wrinkling) wavelength and critical strain in Eq.(3.35) and Eq.(3.37) respectively, the scale factor has not been determined yet. However, the scale factor can be eliminated by considering the ratio of two critical wavelengths or critical strains for two cases with different widths. Such that, model validation is independent of experiment. Due to experiment limitations, it is impossible to measure the critical strain accurately. The validation is only performed for validating the buckling wavelength. The ratio of two critical wavelengths for two systems with different surface film width is expressed as

$$\frac{\lambda}{\lambda_{ref}} = \frac{\sqrt{\alpha_{ref}}}{\sqrt{\alpha}} = \left(\frac{W}{W_{ref}}\right)^{\frac{1}{2}}, \tag{4.1}$$

where α is a function of width. The scale factor c_0 is cancelled out.

Each film width is selected once as reference width W_{ref}. The corresponding buckling wavelength is considered as the reference wavelength λ_{ref}. Ratio of the width, W/W_{ref} or W_{ref}/W, is calculated by using the rest widths divided by the reference width or using the reference width divided by the rest of them. Ratio of the buckling wavelength is obtained follows the same procedure. The dimensionless width W/W_{ref} versus the dimensionless wavelength λ/λ_{ref} is plotted in Figure 4.1 (a)-(f).

Figure 4.1 shows the wrinkling wavelength versus the film width for the analytical model presented in Chapter 3 as well as for the experimental results given in this section. Experimental data in Figure 4.1 has been post-processed in each figure. For each case, the mean value is represented by the quadratic mean obtained via root mean square with an assumption that the error distribution follows Gaussian distribution. Standard deviation has been employed to quantify the error bars. It is
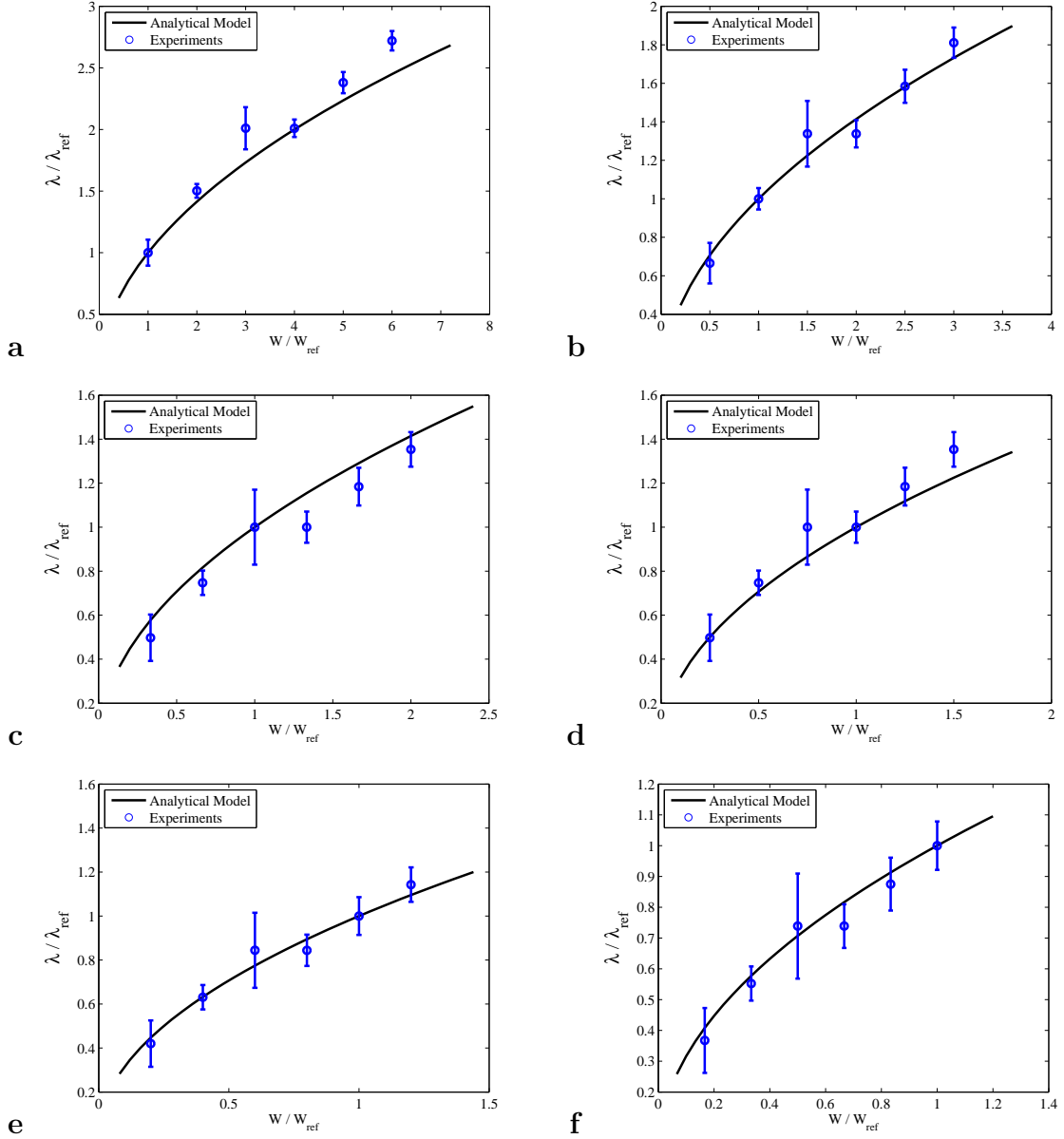
Figure 4.1: Buckling wavelength as a function of the width of surface film, experimental and analytically solution. (a) $W_{ref} = 2.5$ mm, (b) $W_{ref} = 5$ mm, (c) $W_{ref} = 7.5$ mm, (d) $W_{ref} = 10$ mm, (e) $W_{ref} = 12.5$ mm, (f) $W_{ref} = 15$ mm.

observed clearly that the analytical solution agrees with the experimental results in scale.

By defining $\lambda^* = \lambda/\lambda_{ref}$ and $W^* = W/W_{ref}$, it can be observed that

$$\lambda^* = (W^*)^{\frac{1}{2}}. \tag{4.2}$$

Eq.(4.2) is a dimensionless equation which reveals the nature of the finite width effect of the buckling wavelength for the presented problem.

Due to measurement limitations, the lateral compressive strain can not be measured accurately. Therefore, no experimental comparison is provided here. The analytical solution for the ratio of two critical strains is expressed as

$$\frac{\varepsilon}{\varepsilon_{ref}} = \left(\frac{W_{ref}}{W}\right) \tag{4.3}$$

By defining $\varepsilon^* = \varepsilon/\varepsilon_{ref}$, the dimensionless form of Eq.(4.3) which describes the nature of the influence by finite width on critical buckling strain is obtained as

$$\varepsilon^* = \left(\frac{1}{W^*}\right) \tag{4.4}$$

The analytical solution of critical buckling strain ratio as a function of film width ratio is shown in Figure 4.2.

The reference film width selected here follows the same way as shown in the previous figure. Following Tarasovs and Andersons' (2008) work, the x-axis is plotted in log scale. It is seen that critical strain decreases dramatically with the increase of film width. For a narrow film (stripe), the critical strain can be much higher than that of an wide film. The trend observed here is similar to that of Tarasovs and Andersons' (2008) work on buckling of a finite width strip bonded to semi-infinite

elastic foundation.

Therefore, it is clear that the wrinkling profile depends strongly on the film width. Only small compression is needed to generate wrinkles on a relative wide film with finite width. For strip-like thin film on substrate, the model needs to be established carefully with consideration on finite width effect.
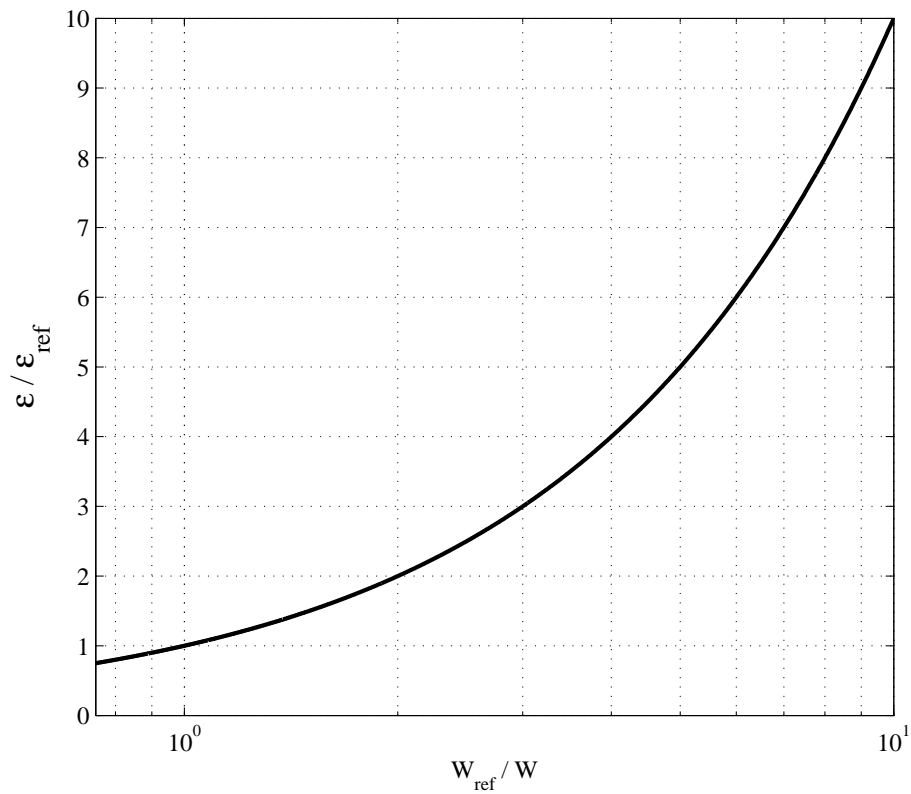

Figure 4.2: Analytical solution of buckling critical strain as a function of the width of surface film.

5. CONCLUSIONS

The presented study investigates the buckling phenomenon of stiff films bonded on stretched thin sheets experimentally and theoretically. Compressive load is provided by lateral contraction due to Poisson effect. Phenomena observed in the experiments include initial wrinkling of the bilayer (buckling) and the wrinkle evolution (post-buckling). The observed behavior of the growth of the wrinkles is very similar to that of the films rested on elastic foundations.

Based on the experimental observations and previous studies, a theoretical model has been developed. The model considers a virtual elastic foundation or an effective elastic foundation on which the composite bilayer rested. The effective stiffness of that elastic foundation is related to the applied load in stretching direction. A scaling analysis is utilized to connect the effective stiffness to the applied load quantitatively. Variational method and principle of minimum potential energy are employed to obtain the governing equation and corresponding buckling wavelength and critical load.

The model also considered finite width effect on the formation of the wrinkle patterns as observed in the experiments. The developed model successfully predicts the buckling wavelength of polyester film on stretched low density polyethylene thin-film. The results agree with the experimental data in scales without additional data fitting.

Further steps may lie in investigating wrinkle evolution and possible delamination. Viscoelastic effect may also need to be addressed in the future works. In addition, influence on wrinkling formation and evolution by pre-stretching may also need to be accounted for the further studies.

REFERENCES

Allen, H., 1969. Analysis and Design of Structural Sandwich Panels. Pergamon Press.

Azevedo, B., Nogueira, L., Marujio, E., Góes, L., Elfes, A., 2011. Operating a network of balloons instead of satellites, in: 11th AIAA Aviation Technology, Integration, and Operations Conference, Virginia Beach, VA.

Biot, M., 1937. Bending of an infinite beam on an elastic foundation. Journal of Applied Mechanics 4, 1–7.

Brau, F., Damman, P., Diamant, H., Witten, T., 2013. Wrinkle to fold transition: influence of the substrate response. Soft Matter 9, 8177–8186.

Brau, F., Vandeparre, H., Sabbah, A., Poulard, C., Boudaoud, A., Damman, P., 2011. Multiple-length-scale elastic instability mimics parametric resonance of nonlinear oscillators. Nature Physics 7, 56–60.

Cao, Y., Hutchinson, J., 2012. Wrinkling phenomena in neo-hookean film/substrate bilayers. Journal of Applied Mechanics 79, 031019 1–9.

Cerda, E., Mahadevan, L., 2003. Geometry and physics of wrinkling. Phys. Rev. Lett. 90, 074302.

Cerda, E., Ravi-Chandar, K., Mahadevan, L., 2002. Wrinkling of an elastic sheet under tension. Nature 419, 579–580.

Chen, X., Hutchinson, J., 2004. Herringbone buckling patterns of compressed thin films on compliant substrate. Journal of Applied Mechanics 71, 597–603.

Chopra, K., Paulson, P., Dutta, V., 2004. Thin-film solar cells: an overview. Progress in Photovoltaics: Research and Applications 12, 69–92.

Chung, J., Nolte, A., Stafford, C., 2011. Surface wrinkling: a versatile platform for

measuring thin-film properties. Advanced Materials 23, 349–368.

Coman, C., 2007. On the applicability of tension field theory to a wrinkling instability problem. Acta Mechanica 190, 57–72.

Davidovitch, B., Schroll, R., Vella, D., Adda-Bedia, M., Cerda, E., 2011. Prototypical model for tensional wrinkling in thin sheets. Proceedings of the National Academy of Sciences of the USA 108, 18227–18232.

Deng, X., 2012. Clefted Equilibrium Shapes of Superpressure Balloon Structures. Ph.d. dissertation. California Institute of Technology.

Groenewold, J., 2001. Wrinkling of plate coupled with soft elastic media. Physica A 298, 32–45.

Hall, J., 2011. A survey of titan balloon concepts and technology status, in: 11th AIAA Aviation Technology, Integration, and Operations Conference, Virginia Beach, VA.

Hall, J., Pauken, M., Kerzhanovich, V., Walsh, G., Fairbrother, D., Shreves, C., Lachenmeier, T., 2007. Flight test results for aerially deployed mars balloons, in: AIAA Balloon Systems Conference, Williamsburg, VA.

van der Heijden, A., 2009. W.T.Koiter's Elastic Stability of Solids and Structures. Cambridge University Press and New York.

Huang, R., 2005. Kinematic wrinkling of an elastic film on a viscoelastic substrate. Journal of Mechanics and Physics of Solids 53, 63–89.

Huang, R., Stafford, C., Vogt, B., 2007. Effect of surface properties on wrinkling of ultrathin films. Journal of Aerospace Engineering 20, 38–44.

Huang, R., Suo, Z., 2002. Wrinkling of a compressed elastic film on a viscous layer. Journal of Applied Physics 91, 1135–1142.

Huang, Z., Hong, W., Suo, Z., 2005. Nonlinear analysis of wrinkles in a film bonded to a compliant substrate. Journal of the Mechanics and Physics of Solids 53,

2101–2118.

Hutchinson, J., 2013. The role of nonlinear substrate elasticity in the wrinkling of thin films. Philosophical Transaction of The Royal Society A 371, 20120422.

Im, S., Huang, R., 2005. Evolution of wrinkles in elastic-viscoelastic bilayer thin films. Journal of Applied Mechanics 72, 955–961.

Jiang, H., D.Y., K., Song, J., Sun, Y., Huang, Y., Rogers, J., 2007. Finite deformation mechanics in buckled thin films on compliant supports. Proceedings of the National Academy of Sciences of the USA 104, 15607–15612.

Jiang, H., Khang, D., Fei, H., Kim, H., Huang, Y., Xiao, J., Rogers, J., 2008. Finite width effect of thin-films buckling on compliant substrate: experimental and theoretical studies. Journal of the Mechanics and Physics of Solids 56, 2585–2598.

Kármán, v., Biot, M., 1940. Mathematical Methods in Engineering. McGraw-Hill.

Khang, D., Jiang, H., Huang, Y., Rogers, J., 2006. A stretchable form of single-crystal silicon for high-performance electronics on rubber substrates. Science 311, 208–212.

Khoury, G., 2012. Airship Technology. Cambridge University Press and New York.

Kim, D., Xiao, J., Song, J., Huang, Y., Rogers, J., 2010. Stretchable, curvilinear electronics based on inorganic materials. Advanced Materials 22, 2108–2124.

Landau, L., Lifshitz, E., 1986. Theory of Elasticity. Pergamon Press.

Lee, H., Kim, D., Cho, I., William, N., Wang, Q., Zheng, X., 2012. Peel-and-stick: fabricating thin film solar cell on universal substrates. Scientific Reports 2, 1–4.

Massabò, R., Gambarotta, L., 2007. Wrinkling of plane isotropic biological membranes. Journal of Applied Mechanics 74, 550–559.

Mei, H., Landis, C., Huang, R., 2011. Concomitant wrinkling and buckle-delamination of elastic thin films on compliant substrates. Mechanics of Materials

43, 627–642.

Nayyar, V., Ravi-Chandar, K., Huang, R., 2011. Stretch-induced stress patterns and wrinkles in hyperelastic thin sheets. International Journal of Solids and Structures 48, 3471–3483.

Pocivavsek, L., Dellsy, R., Kern, A., Johnson, S., Lin, B., Lee, K., Cerda, E., 2008. Stress and fold localization in thin elastic membranes. Science 320, 912–916.

Puntel, E., Deseri, L., Fried, E., 2011. Wrinkling of a stretched thin sheet. Journal of Elasticity 105, 137–170.

Shield, T., Kin, K., Shield, R., 1994. The buckling of an elastic layer bonded to an elastic substrate in plane strain. Journal of Applied Mechanics 61, 231–235.

Song, J., Jiang, H., Liu, Z., Khang, D., Huang, Y., Rogers, J., Lu, C., Koh, C., 2008. Buckling of a stiff film on a compliant substrate in large deformation. International Journal of Solids and Structures 45, 3107–3121.

Steigmann, D., 1990. Tension-field theory. Proceedings of the Royal Society A 429, 141–173.

Sun, J., Xia, S., Moon, M., Oh, K., Kim, S., 2012. Folding wrinkles of a thin stiff layer on soft substrate. Proceedings of The Royal Society A 468, 932–953.

Tarasovs, S., Andersons, J., 2008. Buckling of a coating strip of finite width bonded to elastic half-space. International Journal of Solids and Structures 45, 593–600.

Timoshenko, S., Woinowsky-Krieger, S., 1987. Theory of Plates and Shells. McGraw-Hill.

Vandeparre, H., Piñeirua, M., Brau, F., Roman, B., Bico, J., Gay, C., Bao, W., Lau, C., Reis, P., Damman, P., 2011. Wrinkling hierarchy in constrained thin sheets from suspended graphene to curtains. Physical Review Letters 106, 224301.

Vella, D., Bico, J., Boudaoud, A., Roman, B., Reis, P., 2009. The macroscopic delamination of thin films from elastic substrates. Proceedings of the National

Academy of Sciences of the USA 106, 10901–10906.

Wong, Y., Pellegrino, S., 2006a. Wrinkled membrane part i: Experiments. Journal of Mechanics of Materials and Structures 1, 1–23.

Wong, Y., Pellegrino, S., 2006b. Wrinkled membrane part ii: Analytical models. Journal of Mechanics of Materials and Structures 1, 25–59.

Zang, J., Zhao, X., Cao, Y., Hutchinson, J., 2012. Localized ridge wrinkling of stiff films on compliant substrate. Journal of the Mechanics and Physics of Solids 60, 1265–1279.

Zheng, L., 2009. Wrinkling of Dielectric Elastomer Membranes. Ph.d. dissertation. California Institute of Technology.